Moroccan Journal of Chemistry
ISSN: 2351-812X
http://revues.imist.ma/?journal=morjchem&page=login
xxxx / Mor. J. Chem. 5 N°1 (2017) 120-130

Evaluation of corrosion protection of epoxy coatings on copper during exposure to an aerated 3% NaCl solution.

O. Dagdag[1*], M. El Gouri[1, 3], M. Ebn Touhami[2] and A. El Harfi[1].

[1] *Laboratory of Agroressources, Polymers and process engineering- Team of Organic Chemistry & Polymers, Department of Chemistry, Faculty of Science, University Ibn Tofail, BP 133, 14000 Kenitra, Morocco*

[2] *Laboratory of Materials Engineering and Environment : Modeling and Application, Department of Chemistry, Faculty of Science, University Ibn Tofail, Kenitra, Morocco*

[3] *Laboratory of Process, Renewable Energy and Environment, Department of Process Engineering, Height School of Technology, Sidi Mohammed Ben Abdallah University, Fez, Morocco*

** Corresponding author:*
omardagdagmaster@gmail.com,
Received 10 May 2016,
Revised 15 Jan 2017,
Accepted 30 Mar 2017

Abstract

In this study, the anticorrosion performance of a clear epoxy coating was enhanced by the incorporation of modified zinc into the polymer matrix. Its standard formulation was identified by X-ray diffractometer (XRD). Corrosion performance of the coated copper specimens was investigated employing polarization measurements and electrochemical impedance spectroscopy (EIS) in 3% NaCl solution. Incorporation of 5 wt. % zinc possessed the best corrosion performance. The electrochemical results are completely in agreement with the morphological results of the surface obtained from scanning electron microscopy (SEM). For the theoretical study, complete geometry optimization of 4, 4′- Ethylene bis (N, N diglycidylaniline) was performed using the Density Functional Theory (DFT). The Gaussian 03W software package was used in the calculations.

Keywords: *Epoxy coating, copper, anticorrosion performance, polarization measurements, EIS, SEM and Gaussian 03W.*

1. Introduction

Copper and its alloys are very widely used materials for their excellent electrical and thermal conductivities in many applications such as electronics and integrated circuits. Copper is resistant toward the influence of atmosphere and many chemicals. However, it is susceptible to corrosion in aggressive media, such as Cl^- [1–4]. Organic coatings are the most widely used method of metal bodies protection from atmospheric corrosion. The paint film acts as a physical barrier between corrosive electrolyte and copper substrate. However, it is well known that the coating is permeable to water, oxygen and corrosive ions which are presented in the corrosive electrolyte. Moreover, using organic coatings, the spread of corrosive products will be prevented at the initial sites of electrolyte permeation into the metal surface. Therefore, the adhesion forces which attach the coating to the metal surface can also affect the coating corrosion performance [5-6]. Different parameters including the number of pores, ionic resistance of coating against electrolyte diffusion and the cross-linking density of the coating can affect the coating resistance against electrolyte diffusion through coating matrix. Epoxy is one of the most common barrier coating material used in severe corrosion environments including marine environment [7]. Due to the hydrophilic chemical groups of cured epoxy structure (such as hydroxyl group (–OH), carboxyl group (C=O) and amino group (N–H)), epoxy has exhibited hydrophilic properties [8-9]. This property of epoxy coating causes a negative effect on its protectiveness ability of underneath metal. So therefore, there has been a lot of effort to improve the protectiveness of epoxy coatings, considering their coating thickness and surface treatment methods.

2. Experimental material and procedures

2.1. Tetrafunctional epoxy resins

Tetrafunctional epoxy resin was synthesized by reacting 4, 4′- Ethylene bis (N, N diglycidylaniline) with epichlorohydrin. These epoxy resins have high epoxy functionality and high crosslinking densities [10, 11].

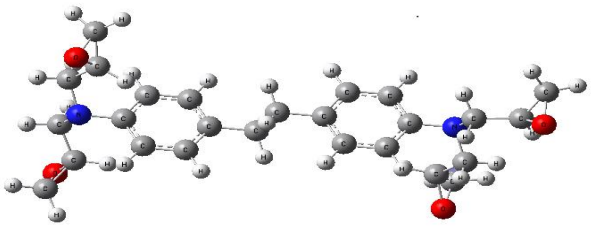

Figure 1: Shows the chemical structure of 4, 4′- Ethylene bis (N, N-diglycidylaniline).

2.2. Amine type curing agent

Amine type curing agents are one of the basic curing agents for epoxy resins, and they can be classified into three major categories: aliphatic, aromatic, or cycloaliphatic amines. Amine type curing agents are one of the basic curing agents for epoxy resins, and they can be classified into three major categories: aliphatic, aromatic, or cycloaliphatic amines. Amine type curing agents react with epoxide rings by nucleophilic addition. We limited ourselves to one hardener class: aromatic amine. According to their chemical structure, add as below [12].

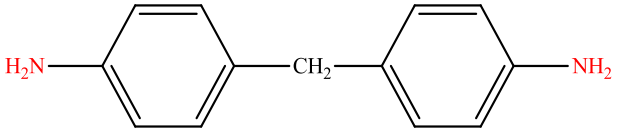

Figure 2: Chemical structure of DDM.

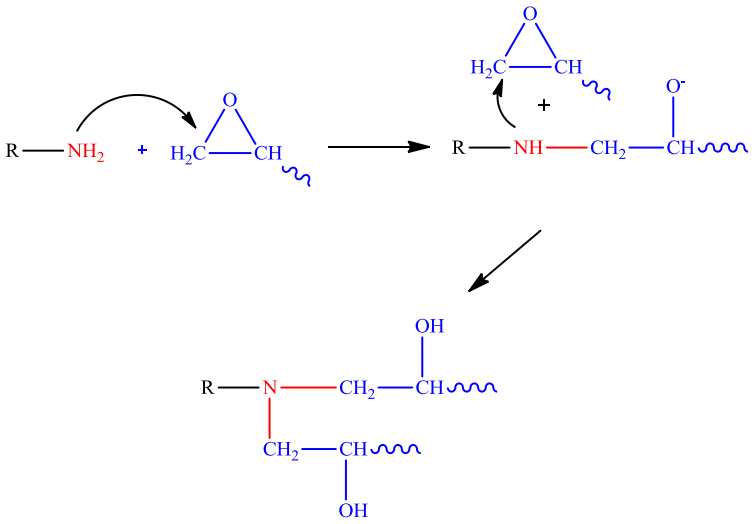

Figure 3: Cure reaction mechanism of amine and epoxide.

2.3. Epoxy-inorganic composites

Several inorganic particles have been added to epoxy resins in order to improve the fracture toughness. Incorporation of inorganic particles leads to an increase in deformation and crack propagation resistance by toughening mechanisms, i.e., particle bridging, crack pinning/bowing, and crack path deflection. The addition of inorganic particles into epoxy resins can increase the modulus, hardness, and fracture toughness [13–15]. Zinc metal particles have been used for many years as ingredients in anticorrosion coating materials.

2.4. Preparation of epoxy resin synthesized formulations

In our study, we proposed new formulation applied on copper which consists of an epoxy resin 4, 4′- Ethylene bis (N, N-diglycidylaniline) synthesized with stoichiometric amounts of the hardening agent (DDM) in the presence of epichlorohydrin as a solvent.

- The different formulations were homogenized in a beaker by mechanical stirring to evaporate the solvent existing in our samples.
- The formulations were applied to carbon steel using a stick that deposits a thickness that varies between 170 ± 10 µm.
- We deposite the coating substrats in an oven for an over night at a temperature of 70° C.

2.5. X-ray diffraction (XRD)

The used apparatus is an XPERT-3 diffractometer with a copper anticathode bombarded by electrons accelerated at a voltage of 45 kV and generating a wavelength of radiation λ ($K\alpha_1$) = 1.54060 A° and λ ($K\alpha_2$) = 1.54443 A°. The equipment is provided with a back monochromator selecting $K\alpha_1$-$K\alpha_2$ doublet. The sample has the form of a film coated on a flat copper support: the incident beam continuously irradiates the flat surface of the sample according to angle θ. The sensor detects the radiation diffracted at an angle 2θ. The various diffraction patterns are stored in vector mode where the angles θ and 2θ are coupled in an angular range in 2θ ranging from 10 ° to 90 ° with a step of 0.04 ° and a count time of 2 sec.

2.4. Evaluation of corrosion-resistant properties of the coating

The morphology of the coatings was characterized using scanning electron microscopy (SEM, JEOL-JSM 5500). The analysis is performed with an acceleration voltage of 0.5-30 kV. The corrosion protection properties of the coatings were tested using pootentiodynamic polarization curves and electrochemical impedance spectroscopy (EIS) measurements, which were performed on Volta lab PGZ100 Potentiostat in a conventional three-electrode cell. The coated carbon steel was used as the working electrode, a large platinum plate used as the counter electrode, and the Ag/AgCl (saturated KCl) electrode was used as the reference electrode. The test solution was a 3 % sodium chloride solution. All tests were conducted at room temperature (25 °C) and open to air. Potentiodynamic polarization curves were obtained by changing the electrode potential automatically from (- 1200 to + 300 mV/Ag/AgCl) versus open circuit potential with a scan rate of 1 mVs^{-1}. EIS measurements were performed over a frequency range of 100 kHz to 0.1 Hz by using a 10 mV amplitude sinusoidal voltage at open cycle potential (OCP). The data were acquired in four cycles at each frequency to obtain good precision at all frequencies. All experiments are performed at the open circuit potential. The obtained impedance data are analyzed in terms of equivalent electrical circuit using Bouckamp's program [16].

2.5. Quantum chemical calculations

The geometry optimization of studied molecule and all quantum chemical calculations have been performed on an Intel based PC. The Gaussian 03W software package was used in the calculations [35]. Density functional theory (DFT) calculations were carried out using Becke's three-parameter functional and the correlation functional of Lee, Yang and Parr (B3LYP) with a 6-31G basis set (without diffuse functions) [17].

3. Results and discussion

3.1. X-rays diffraction

The resulting diagram was recorded at room temperature in a wide angular range $(10° \leq 2\theta \leq 90°)$; with a step of 0.04 ° and a count, time of 2 sec. Figure 4 shows the diffraction pattern of X-rays of the standard formulation MP_1 on the copper after crosslinking. The standard formulation MP_1 after the coated crosslinking on copper exhibits no peaks of XDR characteristics due to the amorphous nature of the polymers [18], and we notice that there is a presence of three lines which are those characterizing the iron and corresponding to the positions 2θ = 43.4° , 50.3° and 73.9°. This is generally observed for amorphous polymers on copper.

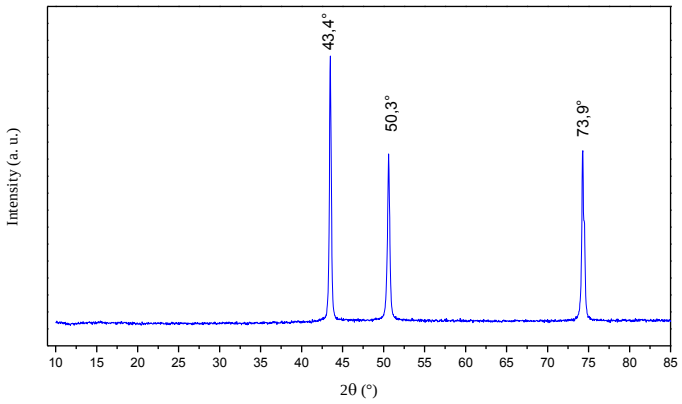

Figure 4: XRD diffractogram of the standard formulation MP_1 after the coated crosslinking on copper.

3.2. Scanning electron microscopy

The surface morphology of copper for the two matrices with standard coating (MP_1) and loaded MP_2 by zinc (Zn) were examined by scanning electron microscopy (SEM) technique as shown in Figure 5. As shown in Fig. 5a, the coating defects due the structural uniformity and integrality of the coating and may degrade for the matrice with standard coating (MP_1). Unlike the matrice loaded MP_2 by zinc (Zn) shows a homogeneous surface (Fig. 5b), which suggests that the well dispersed of the Zn particles better by the epoxy resin.

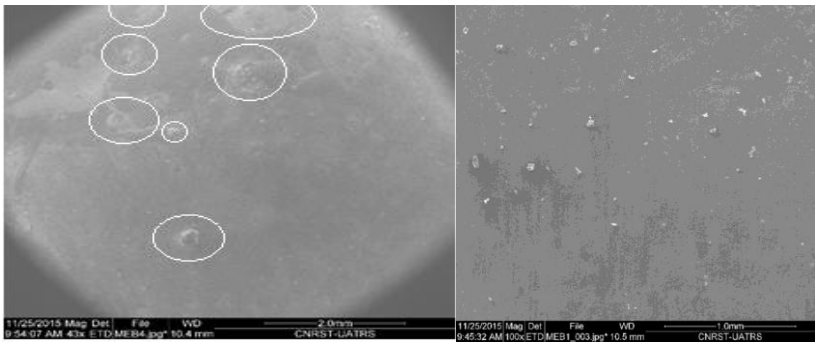

¶ (a) (b)

Figure 5: SEM images (a) and (b) of copper surface for the two matrix with standard coating (MP_1) and loaded (MP_2).

3.3. Potentiodynamic polarization measurements

Figure 6 shows the polarization curves of the copper at different matrices in artificial sea water (3% NaCl). The corrosion parameters determined from these curves are listed in Table 1. Table 1 illustrates some parameters such as corrosion potential, E_{corr}, corrosion current density, i_{corr}, anodic and cathodic Tafel slopes, β_a, β_c and efficiency of protection η (%). The corrosion efficiency of protection is determined by the following equation (1) [19]:

$$\eta = \frac{i^0_{corr} - i_{corr}}{i^0_{corr}} \times 100 \quad (1)$$

where i^0_{corr} and i_{corr} are respectively the current densities of the corrosion of the steel tempered in the corrosive medium with and without a coating of various formulations, which are obtained by the extrapolation of cathodic and anodic Tafel right to the corrosion potential.

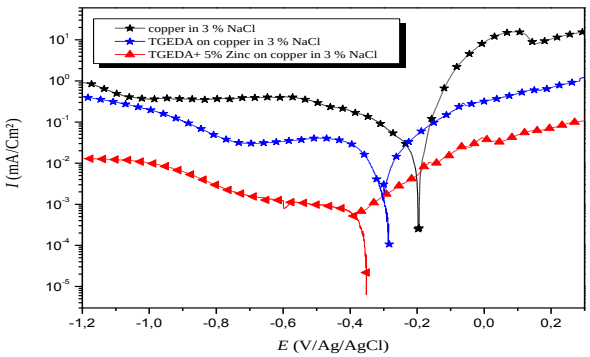

Figure 6: Potentiodynamic polarization curves for copper in 3% NaCl solutions without and with different matrices after immersion for 40 min at 298 K.

Table 1. Electrochemical parameters for the copper electrode in 3% NaCl with and without a coating of various formulations.

Plates	E_{corr} (mV/Ag/AgCl)	i_{corr} (µA/cm²)	$-\beta_c$ (mV/dec)	β_a (mV/dec)	η %
MP_0	-190	24	391	325	-
MP_1	-282	2.4	451	230	90
MP_2	-353	0.9	344	205	96.5

3.4. The analysis and interpretation of results:

The protection mechanism is studied in this paragraph according to the protective matrices which are constituted by the standard polymeric epoxy resin MP_1 and zinc as additive (MP_2). The interpretation of the results according to the constitution of the matrix is given as follows and regrouped in figure 7. In the matrix MP_0 as a witness which is constituted without a substrate coating (copper), anions Cl^- and OH^- from the corrosive environment directly attack the substrate which indicates a direct and increased corrosion (Figure 7). Through the MP_1 matrix, we expect that there is a relatively large diffusion of chloride ions and hydroxide through the protective film, which may present micropores, while inducing a primary corrosion. This would lead to an acceleration of the anodic dissolution of the metal (Figure 8) [20].

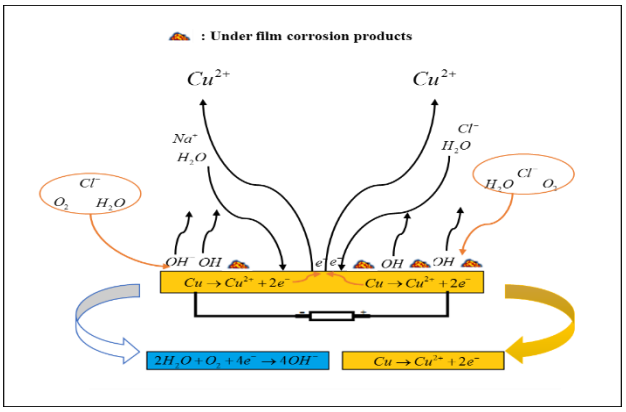

Figure 7: Mechanism proposed for the matrix MP_0 as a witness, which is constituted without a substrate coating (copper) after the immersion in 3% NaCl.

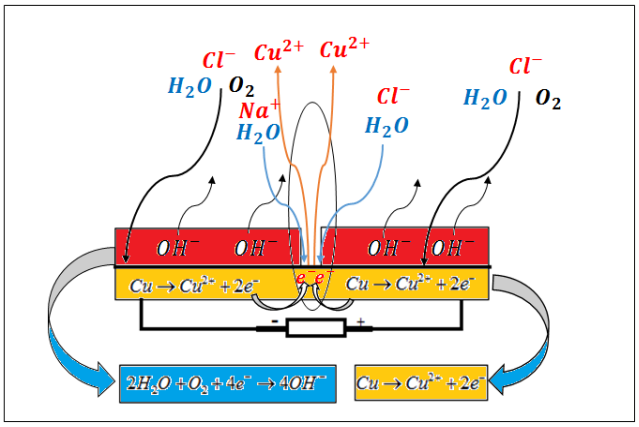

Figure 8: Mechanism proposed for the protective matrix MP_1 between the metal substrate and the film after the immersion in 3% NaCl.

On this basis, the coating with the matrix MP_2 indicates the diffusion of corrosive species $(Cl^-$ *and* $OH^-)$ is slowed by the coating of passivation from the couple Zn/Zn^{2+} according to equations 2 and 3 (Figure 9).

$$Zn^{2+} + 2OH^- \longrightarrow Zn(OH)_2 \longrightarrow ZnO + H_2O \quad (2)$$

$$Zn^{2+} + 2Cl^- \longrightarrow Zn(Cl)_2 \quad (3)$$

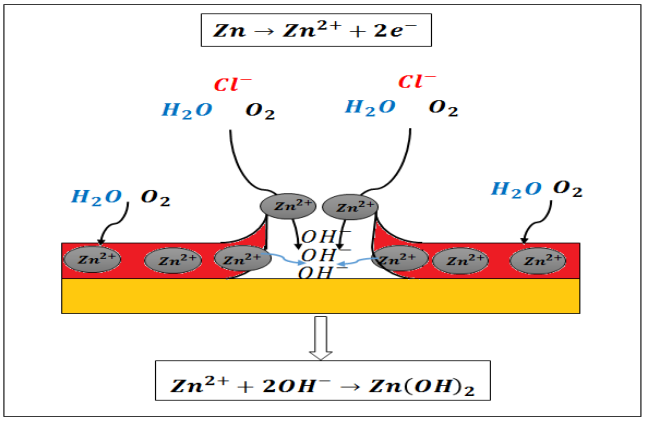

Figure 9: Mechanism of formation of the passivation coating at the interface between the metal substrate and the film after the immersion in 3% NaCl.

3.5. Electrochemical impedance spectroscopy (EIS) measurements.

The impedance diagrams of these copper products, which are immersed for 40 minutes before each measurement in an open circuit in the corrosive solution 3% NaCl vis-a-vis all matrices are grouped in Figure 10. The analysis of the different diagrams corresponding respectively to the protective matrices shows that the latter are formed by two capacitive loops: one with high frequency (HF) assigned to the film effect and the other with low frequency (LF) which is generally attributed to the charge transfer process. This is due to the phenomenon diffusion. Indeed, the larger the diameter of semicircle longer increases, the better will be the corrosion resistance of the protective film.

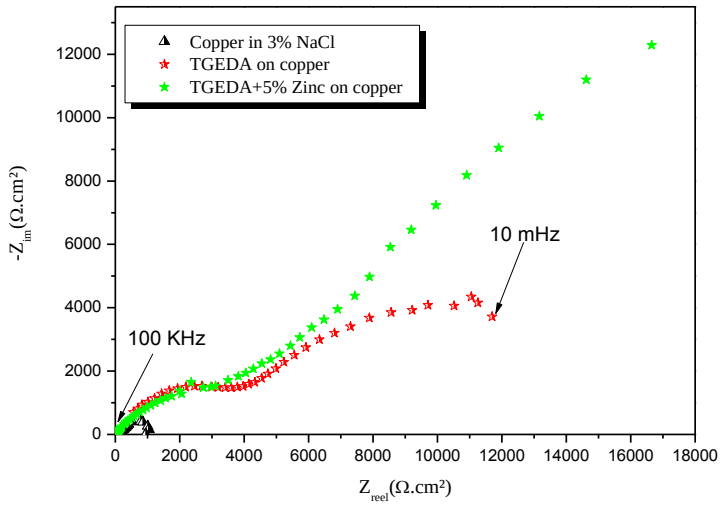

Figure 10: Electrochemical impedance diagrams with open circuit after 40 min of immersion for copper in 3% NaCl in the presence of matrices MP_1 and MP_2 at 298 K.

For the electrochemical impedance spectroscopy results, we based our study on the equivalent circuit established in figure 11. This circuit is composed of : R_s which is the resistance of the electrolyte ($\Omega.cm^2$) ; R_{pf} which is the resistance

of the coating pores ; R_{pf} which corresponds to the diameter of the first semi-circle at high frequencies of the diagram Nyquist ; R_{ct} which is the charge transfer resistance ; C_f which is the di-electric capacity of the coating film ; and C_{dl} which is the double layer capacity of the substrate. The value of the efficiency of protection (η %) is evaluated from R_p which is obtained from the diameter of the semi-circle in the Nyquist representation that was found by using equation (4) :

$$\eta = \frac{R_p - R_p^{\circ}}{R_p} \times 100 \quad (4)$$

where R_p and R_p^0 are respectively the resistance with and without a coating. The values of electrochemical impedance and the protective efficiency resulting from each matrice of protection MP_1 and MP_2 are summarized in Table 2.

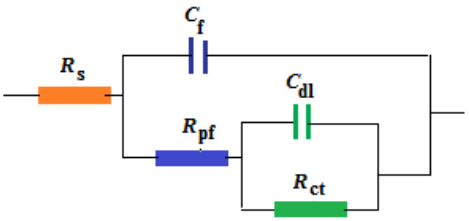

Figure 11: Electrical equivalent circuit for the studied coating systems.

Table 2. Different electrochemical parameters extracted by EIS measurements.

Plates	R_s (Ω.cm²)	C_f (µF/cm²)	R_{pf} (Ω.cm²)	C_{dl} (µF/m²)	R_{ct} (Ω.cm²)	R_p (Ω.cm²)	η %
MP_0	20	-	-	-	950	1200	-
MP_1	540	41.5	1950	18.62	13830	15240	92%
MP_2	638	30.09	2700	5.02	44160	46222	97%

This table shows that the values of the polarization resistance (R_p) for the four coating matrices are evaluated between 15.10^3 and 44.10^3 Ω.cm². On this basis, the largest semi-circle in the Nyquist diagram of MP_2 coating system indicates a better corrosion resistance, which can be explained by the presence of the Zinc responsible for higher corrosion resistance.

3.6. Scanning electron microscopy

To confirm the results obtained by the electrochemical measures for the two matrices with standard coating (MP_1) and loaded (MP_2) by zinc (Zn), we used as a means of analysis the coating surface on copper in 3% NaCl after the immersion for 48 hours at 298 K.. Figure 12 shows the SEM morphologies of the state of copper surface immersed in 3% NaCl for 48 h at 298 K.

The standard protective matrix MP_1 submerged the immersion for 48 hours in a 3% NaCl solution. As shown in figure 12 (a), we expect that there is a relatively spread of electrolytes (chloride ions) through the protective film which may present micropores / defects. In addition, the SEM micrography during the application of the MP_2 matrix in figure 12 (b), we observed in the film surface of the coating some white spots considered as corrosion products according to the literature and this shows that it is concerned with the zinc oxide layer which is necessary for the protection of metals.

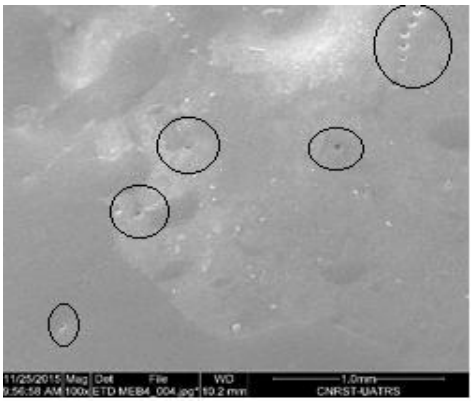

(a)

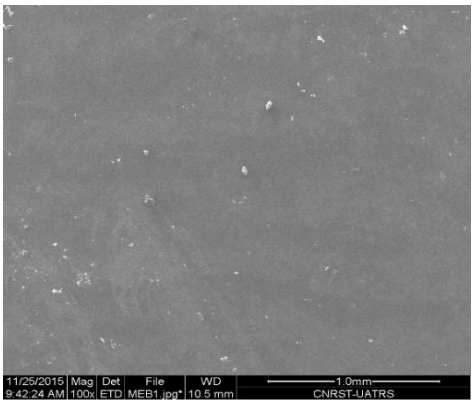

(b)

Figure 12 : SEM images (a) and (b) of copper surface for the two matrices with standard coating (MP_1) and loaded MP_2 by zinc (Zn) after the immersion for 48 hours in 3% NaCl.

3.7. Quantum chemical calculations

Corrosion protection ability of conducting polymer coatings depends on both structural and electronic properties. It was shown in the literature that useful knowledge about electronic character of a conducting polymer could be obtained by DFT calculations. The effectiveness of a particular donor/acceptor can be assessed by computation of certain quantum chemical parameters such as the energy of the highest occupied molecular orbital (E_{HOMO}), the energy of the lowest unoccupied molecular orbital (E_{LUMO}) and LUMO-HOMO gap (E_{LUMO}-E_{HOMO}). E_{HOMO} is a quantum chemical descriptor, which is often associated with the electron donating ability of the molecule. High value of E_{HOMO} indicates the tendency of a molecule to donate electrons to an appropriate acceptor molecule with empty molecular orbitals. Therefore, the energy of E_{LUMO} indicates the ability of a molecule to accept electrons. On the other hand, values of energy gap ($\Delta E = E_{LUMO} - E_{HOMO}$) is the measure of excitation energy to remove an electron from the last occupied molecular orbital. Hence, an increase in the values of E_{HOMO} can facilitate the disposition of the molecule to donate orbital electrons to an appropriate acceptor and decrease in E_{LUMO} is an indication of strong interaction with metal. Low values of $E_{LUMO} - E_{HOMO}$ will provide good coating efficiencies.

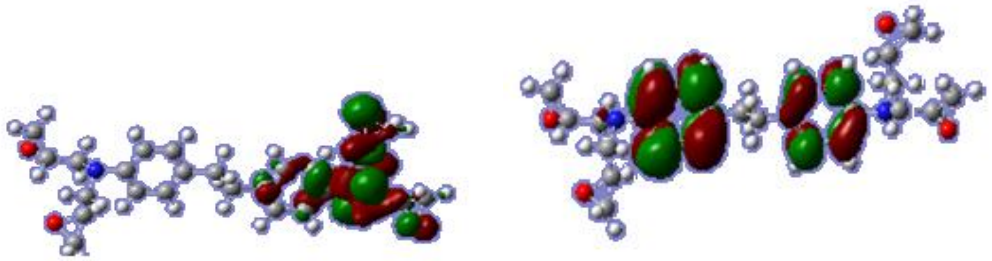

E_{HOMO}

E_{LUMO}

Figure 13: HOMO and LUMO population of the 4, 4′- Ethylene bis (N, N diglycidylaniline).

According to the frontier molecular orbital theory, the density distribution of HOMO is very critical in order to distinguish the adsorption center of the protection molecules, which are responsible for the interaction with the metal surface.

It can be seen from Fig. 13 that, HOMO is extensively distributed over large central part of the 4, 4′- Ethylene bis (N, N diglycidylaniline). However, LUMO distribution locates on just one side and small part of the 4, 4′- Ethylene bis (N, N diglycidylaniline). When the HOMO is extensively distributed on larger part of epoxy resin, the epoxy resin is preferentially well adsorbed onto metal surface. Distribution of HOMO energy at one side and small region of molecule causes adsorption of smaller part of polymer onto the metal surface. Adhesion is an important problem to be considered in the corrosion protection of metals by conducting polymer coatings. Our experimental results show that the 4, 4′- Ethylene bis (N, N diglycidylaniline) has the best protective performance for the corrosion of copper in 3 % NaCl solution. HOMO distribution of epoxy resin quite well support the experimental corrosion performance of studied 4, 4′- Ethylene bis (N, N diglycidylaniline). The computed quantum chemical parameters like E_{HOMO}, E_{LUMO} and $\Delta E_{LUMO-HOMO}$ of the 4, 4′- Ethylene bis (N, N diglycidylaniline) are summarized in Table 3.

Table 3. E_{HOMO}, E_{LUMO} and $E_{LUMO-HOMO}$ values of the studied 4, 4′- Ethylene bis (N, N diglycidylaniline).

Molecule	E_{HOMO}	E_{LUMO}	$\Delta E_{LUMO-HOMO}$
4,4′- Ethylene bis (N, N diglycidylaniline)	- 0,336	- 0,192	0,144

4. Conclusion

In this study, we carried out the protection of the copper by the coating method issued from the formulations which are based on a standard oxide polymer (MP_1) and zinc inorganic filler (MP_2). This was done in order to decrease the corrosive effect of the medium on the copper. The main findings of this study can be drawn as follow:

- The corrosion protective effect of the formulated matrix MP_2 gave us the best results.
- The SEM observation shows that the surface of the matrix based on a polymer loaded with zinc deposited on copper completely protected is due to the formation of a protective layer which limits the penetration of electrolyte through the protective film.
- Parameters calculated of studied 4, 4′- Ethylene bis (N, N diglycidylaniline) were found to be well correlated with experimental order of corrosion performances of the coatings.

References

[1] Wang, D., Xiang, B., Liang, Y., Song, S., & Liu, C., *Corros. Sci*. *85* (2014) 77.

[2] Peng, S., Zhao, W., Li, H., Zeng, Z., Xue, Q., & Wu, X., *Appl. Surf. Sci*. *276* (2013) 284.

[3] Chang, H. C., Lin, H. T., Lin, C. H., & Su, W. C., *Poly. Degrad. Stab*. *98* (2013) 102.

[4] Montemor, M. F., *Surf. Coat. Tech*. *258* (2014) 17.

[5] Singh-Beemat, J., & Iroh, J. O., *Prog. Org. Coat*. *74* (2012)173.

[6] Kumar, S. A., & Sasikumar, A., *Prog. Org. Coat*. *68* (2010) 189.

[7] Yu, Z., Di, H., Ma, Y., Lv, L., Pan, Y., Zhang, C., & He, Y., *Appl. Surf. Sci*. *351* (2015) 986.

[8] Dagdag, O., Galai, M., Touhami, M. E., El Harfi, A., *Inter. J. of Innov. Appl. Stud*. 1 (2015) 295.

[9] Park, S. J., Jin, F. L., & Lee, J. R., *Mat. Sci. Engineer. A*. 1 (2004) 109.

[10] Lee, M. C., Ho, T. H., & Wang, C. S., *J. of Appl. Poly. Sci*. 1 (1996) 217.

[11] Ferdosian, F., Ebrahimi, M., & Jannesari, A., *Thermochimica Acta*. *568* (2013) 67.

[12] Park, S. M., Lim, Y. W., Kim, C. H., Kim, D. J., Moon, W. J., Kim, J. H., Seo, G., *J. of Indus. Engineering Chem*. 2 (2013)712.

[13] Hwang, S. S., & Hsu, P. P., *J. of Indus. Engineer. Chem*. 4 (2013) 1377.

[14] Lim, C. W., Song, K., & Kim, S. H., *J. of Indus. Engineer. Chem*. 1 (2012) 24.

[15] Dagdag, O., El Gouri, M., Galai, M., Touhami, M. E., Essamri, A., & Elharfi, A., *Der Phar. Chem*. 4 (2015) 284.
[16] Frisch, M. J., Trucks, G.W., Schlegel, H. B., Scuseria, G. E., Robb, M. A., Cheeseman, J. R., Montgomery J. A., Vreven, T., Kudin, K. N., Burant, J. C., Millam, J. M., Iyengar, S. S., Tomasi, J., Barone, V., Mennucci, B., Cossi, M., Scalmani, G., Rega, G., Petersson, A., Nakatsuji, H., Hada, M., Ehara, M., Toyota, K., Fukuda, R., Hasegawa, J., Ishida, M., Nakajima, T., Honda, Y., Kitao, O., Nakai, H., Klene, M. X., Li, J.,E., Knox, H. P., Hratchian, J. B., Cross, V., Bakken, C. Adamo, J., Jaramillo, R., Gomperts, R. E., Stratmann, O., Yazyev, A. J., Austin, R., Cammi, C., Pomelli, J. W. Ochterski, P. Y., Ayala, K., Morokuma, G. A., Voth, P., Salvador, J. J., Dannenberg, V. G., Zakrzewski, S., Dapprich, A. D., Daniels, M. C., Strain, O., Farkas, D. K., Malick, A. D., Rabuck, K., Raghavachari, J. B., Foresman, J. V., Ortiz, Q., Cui, A. G., Baboul, S., Clifford, J., Cioslowski, B. B., Stefanov, G. Liu, A. Liashenko, P. Piskorz, I. Komaromi, R. L. Martin, D. J. Fox, T. Keith, M. A., Al-Laham, C. Y., Peng, A., Nanayakkara, M. Challacombe, P .M. W., Gill, B. Johnson, W. Chen, M. W., Wong, C., Gonzalez, J. A., Pople, Gaussian 03W, Revision C.02, Gaussian, Inc., 340 Quinnipiac Street, Building 40, Wallingford, CT, 06492, 2004, (Copyright C 1994–2003).
[17] O. Dagdag and A. El Harfi., *J. Chem. Pharmac. Res*. 11 (2015) 75.
[18] Hao, Y., Liu, F., Han, E. H., Anjum, S., & Xu, G., *Corros. Sci*. *69* (2013) 77.
[19] Zubielewicz, M., & Gnot, W., *Prog. Org. Coat*. 4 (2004) 358.
[20] Masoud, M. S., Awad, M. K., Shaker, M. A., & El-Tahawy, M. M. T., *Corros. Sci*. 7 (2010) 2387.